

## Independent superconductivity and paramagnetism in $\text{HoBa}_2\text{Cu}_3\text{O}_z$

J. R. Thompson

*Solid State Division, Oak Ridge National Laboratory, Oak Ridge, Tennessee 37831-6061  
and Department of Physics, University of Tennessee, Knoxville, Tennessee 37996-1200*

D. K. Christen, S. T. Sekula, B. C. Sales, and L. A. Boatner

*Solid State Division, Oak Ridge National Laboratory, Oak Ridge, Tennessee 37831-6061  
(Received 20 April 1987)*

The magnetic properties of the superconductive materials  $\text{HoBa}_2\text{Cu}_3\text{O}_z$  and  $\text{YBa}_2\text{Cu}_3\text{O}_z$  have been measured and compared. Both had superconductive transition temperatures  $T_c$  in low magnetic fields near 90 K and exhibited nearly complete magnetic-flux exclusion. The susceptibility of the Ho-based material followed a Curie-Weiss law both above and below  $T_c$ . These results give clear experimental evidence for a nearly complete decoupling of the magnetic and superconductive layers, demonstrating that the superconductivity is highly anisotropic.

### INTRODUCTION

Since the report by Bednorz and Müller<sup>1</sup> of superconductivity above 30 K, there has been an explosive growth of activity in this area. To date, all of the materials possessing superconductive transition temperatures  $T_c > 30$  K have been oxygen-deficient copper-oxide-based compounds of the type  $R_xA_y\text{CuO}_z$ . Here  $A$  represents a divalent alkaline-earth element (Ba, Sr, . . .) and  $R$  is a trivalent element, including Y, La, and the rare-earth elements. Structurally, the materials are based on modified perovskites: The family of compounds<sup>2</sup> with  $T_c \approx 35$  K, typified by  $\text{La}_{1.85}\text{Sr}_{0.15}\text{CuO}_4$ , have tetragonal unit cells with a  $\text{K}_2\text{NiF}_4$  structure.<sup>3,4</sup> Materials with higher  $T_c$ 's  $\approx 90$  K (Ref. 5), such as  $\text{Y}_1\text{Ba}_2\text{Cu}_3\text{O}_z$ , are orthorhombic, wherein the basal cell lengths  $a$  and  $b$  differ slightly.<sup>6</sup> (Generically we refer to these as "1-2-3" compounds.) A very important feature common to both sets of materials is the presence of Cu-O sheets. In band-structure calculations<sup>7</sup> for  $\text{K}_2\text{NiF}_4$ -structured compounds, the essentially two-dimensional (2D) character of the associated electronic states has been emphasized. Weber<sup>8</sup> has attributed additional importance to these states with the theoretical result that quite strong electron-phonon coupling arises almost entirely from breathing mode oscillations in the layered Cu-O complex; coupling to the surrounding layers containing trivalent species is virtually nonexistent.

If the important electronic states are indeed very strongly localized in one direction, this will greatly modify many material properties, both normal and superconductive. Furthermore, technical applications exploiting the superconductivity may be quite seriously impacted. Thus it is extremely important to obtain experimental evidence for strong decoupling between Cu-O and  $R$  layers. The first experimental indication of this came with the observation<sup>9</sup> that if trivalent rare-earth ions, e.g., Gd, Eu, etc., were substituted for nonmagnetic  $\text{Y}^{3+}$ , the resulting "1-2-3" materials were still superconductive with  $T_c$  values near 90 K. Since local magnetic moments are normally quite effective superconductive pair breakers, this obser-

vation implies that the pairs effectively avoid the layers containing rare-earth elements.

In this work, we provide much stronger experimental evidence for strongly two-dimensional superconductive layers in the "1-2-3" materials. When substituted for Y, the rare-earth ions retain their local moments and *can be readily magnetized by an applied magnetic field, even in the superconductive state at temperatures well below  $T_c$* . This is demonstrated by magnetization and magnetic susceptibility investigations of  $\text{Ho}_1\text{Ba}_2\text{Cu}_3\text{O}_z$  between 4.2 and 290 K. Similar measurements on  $\text{Y}_1\text{Ba}_2\text{Cu}_3\text{O}_z$  provide a baseline for comparison.

### EXPERIMENTAL ASPECTS

The samples investigated were synthesized by reaction and sintering of cold-pressed pellets. The resulting Ho-based pellets were hard, relatively dense ( $\rho = 5.4 \text{ g/cm}^3$  obtained from sample geometry), and black; the Y-based ones were also black, somewhat softer, with a lower relative density ( $\rho = 3.7 \text{ g/cm}^3$ ). To begin, appropriate amounts of  $\text{Ho}_2\text{O}_3$ ,  $\text{BaCO}_3$ , and  $\text{CuO}$  powders were thoroughly mixed and placed in an alumina boat in an atmosphere of flowing oxygen. The powder was fired at 895°C for about 20 h and then reground. The grinding was accomplished by making a methanol-powder slurry which was loaded into an automatic powderizing chamber containing agate cylinders. After drying, the finely ground powder was again refired at 895°C for 20 h. The entire firing and grinding process was repeated three times to ensure completely homogeneous powder. The prereacted powder was cold pressed into 1.25 cm by 0.3-cm-thick cylinders at a pressure of 500 bars and placed in a platinum boat in an atmosphere of flowing oxygen. The cold-pressed pellets were heated at 2°C/min to 945°C, held at 945°C for 16 h, cooled at 0.5°C/min to 500°C, after which the furnace was turned off. Powder x-ray diffraction analysis of the resulting ceramics indicated that the material was single phase (< 5% impurity phase) and of the same structure as  $\text{Y}_1\text{Ba}_2\text{Cu}_3\text{O}_7$ .<sup>6</sup>

The magnetic investigations were performed in a vibrating sample magnetometer equipped with a superconductive solenoid. Applied magnetic fields to 80 kOe were utilized over a temperature range of 4.2–290 K. The field was applied parallel to the long axis of the plate- or disk-like samples in order to minimize demagnetizing effects. Sample temperature was measured in zero field with a calibrated Si diode (checked against liquid N<sub>2</sub> vapor pressure) and controlled with a field-insensitive carbon glass thermometer. In the superconductive state, data were acquired as isothermal magnetization curves, while the normal-state susceptibility was acquired by sweeping the temperature in a constant magnetic field of 10.8 kOe.

### EXPERIMENTAL RESULTS

The transition temperature  $T_c$  of the Ho<sub>1</sub>Ba<sub>2</sub>Cu<sub>3</sub>O<sub>2</sub> sample, measured magnetically, was 86.6 K (midpoint) and 90.0 K when 90% in the normal state. The corresponding values for the Y-based material were 88.0 and 91.5 K, respectively. After cooling to 4.2 K in zero magnetic field (ZFC), flux exclusion exceeding 90% of the ideal Meissner diamagnetism was observed. This baseline was used in determining the  $T_c$  value given above. As shown in Fig. 1, the electrical resistivity  $\rho$  of the Ho-based sample is metallic with a linear temperature dependence initially. It decreases from 1000 to 400  $\mu\Omega$  cm as the temperature decreases from 295 to 100 K. Measured resistively, the  $T_c$  midpoint is 91.5 K with zero resistivity at 90.2 K. The similarity of  $T_c$  values from the inductive onset (90.0 K) and zero resistivity measurements is indicative of relatively high homogeneity for both the Ho- and Y-based samples.

The magnetic susceptibility  $\chi$  of Y<sub>1</sub>Ba<sub>2</sub>Cu<sub>3</sub>O<sub>2</sub> is presented first so that the results can be used below. Figure 2 shows the cgs dimensionless (volume) susceptibility  $\chi$  versus inverse temperature. (Note that the geometrical volume, not that obtained from the x-ray density, has been used.) The solid line in Fig. 2 has been fitted to the Curie law relation

$$\chi = \chi_0 + C/T, \quad (1)$$

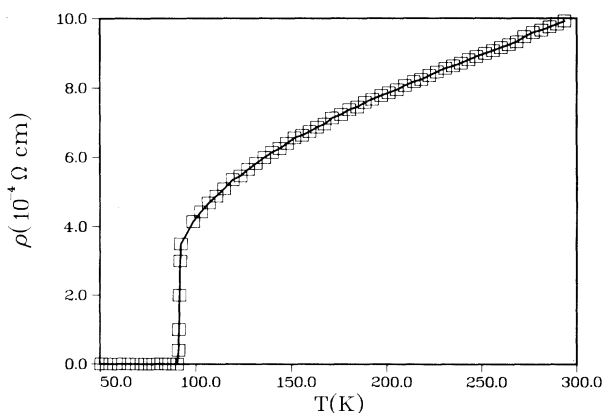


FIG. 1. The electrical resistivity  $\rho$  (in units of  $10^{-4} \Omega \text{ cm}$ ) vs temperature  $T$  for Ho<sub>1</sub>Ba<sub>2</sub>Cu<sub>3</sub>O<sub>2</sub>. The midpoint of the superconductive transition is 91.6 K.

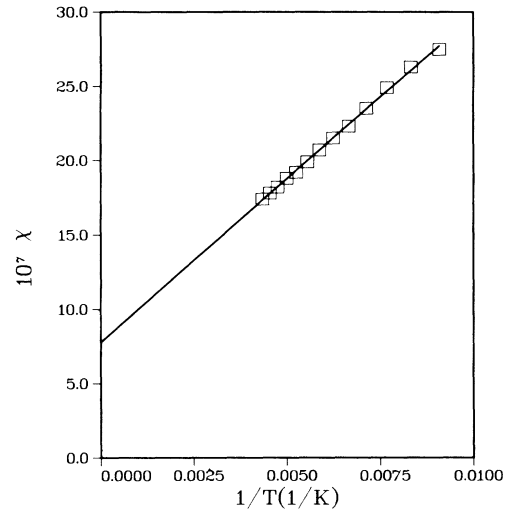


FIG. 2. The cgs volume susceptibility  $\chi$  of Y<sub>1</sub>Ba<sub>2</sub>Cu<sub>3</sub>O<sub>2</sub> vs inverse temperature ( $1/T$ ). The sample mass and volume are 0.2377 g and 0.064 cm<sup>3</sup>, respectively.

yielding a temperature-independent value  $\chi_0 = 7.78 \times 10^{-7}$  (cgs) =  $1.39 \times 10^{-4}$  cm<sup>3</sup>/mole. The Curie constant  $C = Np^2\mu_B^2/3k_B$  is  $2.19 \times 10^{-4}$  K =  $3.91 \times 10^{-2}$  K cm<sup>3</sup>/mole, where 1 mole refers to  $6.02 \times 10^{23}$  units of Y<sub>1</sub>Ba<sub>2</sub>Cu<sub>3</sub>O<sub>6.9</sub>. If the temperature dependence is attributed solely to the copper, one obtains an effective moment  $p = 0.3\mu_B/\text{Cu}$  ion, in agreement with the determination of Cava, Batlogg, and van Dover.<sup>6</sup>

We turn now to the results for the Ho-based material, Ho<sub>1</sub>Ba<sub>2</sub>Cu<sub>3</sub>O<sub>2</sub>. Since the Ho ions are expected to interact strongly, we analyze  $\chi$  for  $T > T_c$  using the Curie-Weiss relation

$$\chi = \chi_0 + C/(T + \Theta), \quad (2)$$

where  $\Theta$  is the Curie-Weiss temperature. (In this case,  $\chi_0$  is extremely small relative to the temperature-dependent Ho paramagnetism; we have therefore used the molar  $\chi_0$  value found for Y-based material, but this assumption does not affect the following analysis.) Accordingly, Fig. 3 is a plot of  $1/(\chi - \chi_0)$  vs  $T$ . The straight line per Eq. (2) has been fitted to the data for the temperature interval  $T > T_c$ , yielding  $\Theta = +13$  K. From the slope, an effective moment per Ho<sup>3+</sup>,  $p = [g^2J(J+1)]^{1/2}$ , of  $10.6\mu_B$  is obtained, which is precisely that expected for a <sup>5</sup>I<sub>8</sub> ion.

There is one feature in Fig. 3 which is extremely important: The  $\chi$  data well below  $T_c$  lie quite close to the Curie-Weiss line obtained from the data above  $T_c$ . Thus the field-induced paramagnetism and superconductivity (which is assured since the applied field is much smaller than the upper critical field  $H_{c2}$ ) are occurring quite independently of one another. Stated differently, this result gives strong support to the idea discussed above that the superconductive electron pairs are localized in sheets that do not contain Ho ions.

Further evidence supporting this conclusion can be found in low-temperature magnetization data, which show a superposition of superconductive and high-field para-

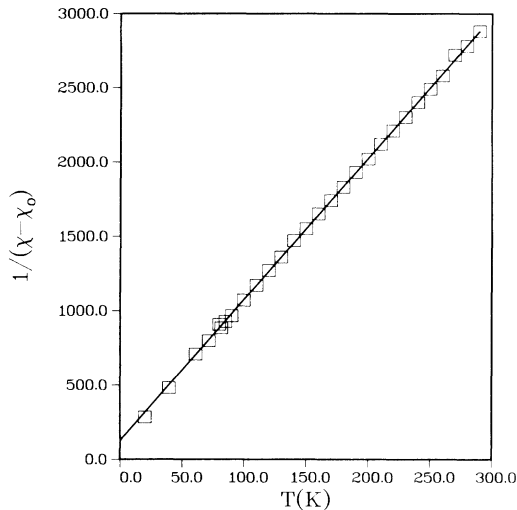


FIG. 3. The inverse of the temperature-dependent volume susceptibility of 4  $\text{Ho}_1\text{Ba}_2\text{Cu}_3\text{O}_z$  vs temperature  $T$ . The Curie-Weiss response is unaffected by the superconductive transition near 90 K.

magnetic behavior. Figures 4 and 5 are plots of the irreversible magnetization of  $\text{Ho}_1\text{Ba}_2\text{Cu}_3\text{O}_z$  at 20 and 4.2 K, respectively, obtained in increasing and decreasing magnetic field. There are several noteworthy features. As the field is first increased, there is a low-field diamagnetic peak typical of type-II superconductors. Also typical is the hysteresis evident upon field reversal at 79 kOe. What is quite unusual is that this superconductive magnetization is superpositioned atop an enormous, saturating paramagnetism arising from the Ho ions. Because of their interactions, however, the paramagnetic ions saturate more slowly than predicted by a standard Brillouin function  $B_J(g\mu_B JH/k_B T)$ .

We can, to a first approximation, allow for the substantial interaction strength by modifying the Brillouin func-

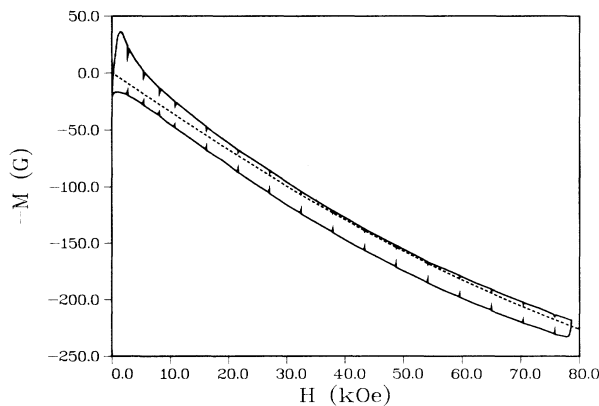


FIG. 4. The magnetization  $-M$  vs applied field  $H$  for  $\text{Ho}_1\text{Ba}_2\text{Cu}_3\text{O}_z$  at  $T=20$  K. Data are shown for increasing and decreasing field. The broken line is a Brillouin function modeling at an effective temperature  $(T + \Theta_M) = 31$  K.

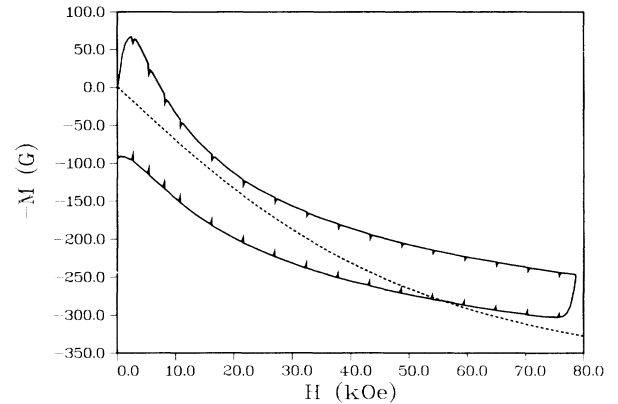


FIG. 5. Magnetization (as Fig. 4) of  $\text{Ho}_1\text{Ba}_2\text{Cu}_3\text{O}_z$  at  $T=4.2$  K. The broken line is calculated using  $(T + \Theta_M) = 15$  K.

tion as suggested by the Curie-Weiss susceptibility. As a model relation, we write

$$M(H, T) = M_{\text{sat}} B_J(g\mu_B JH/k_B [T + \Theta_M]) , \quad (3)$$

where  $\Theta_M$  should be similar in magnitude to the  $\Theta$  value obtained from the high-temperature susceptibility.

The results of this modeling can be seen in Figs. 4 and 5 as the dashed lines. For  $\Theta_M$ , a value of +11 K has been chosen; this and all other values used ( $g=1.25$ ,  $J=8$ ) are entirely consistent with the susceptibility data.

For the magnetization data at 20 K in Fig. 4, it is evident that the saturating Ho magnetism is described reasonably well in this way. Use of the model with the same  $\Theta_M$  value for data at 4.2 K gives less satisfactory agreement; however, with  $T < \Theta_M$  and with most implicit mathematical approximations violated, it is noteworthy that this representation works as well as it does. In addition, very similar values for  $\Theta$  and  $\Theta_M$ , 13, and 11 K, respectively, have been obtained, which lends further credence to the modeling.

The positive values for  $\Theta$  and  $\Theta_M$ , simulating antiferromagnetism, are likely to arise from a combination of the magnetic dipolar interaction and crystal-field effects, which ultimately produce a singlet ground state in  $\text{Ho}^{3+}$ . For Ho ions in a nearly square planar array, the dipolar interaction between two near neighbors is  $\sim 1$  K. Summed over neighbors, this alone becomes quite comparable with the  $\Theta$  values obtained, so dipolar interactions must contribute very significantly to the difficulty of magnetizing the Ho moment system at low temperature.

In addition to paramagnetism of the Ho subsystem, Figs. 4 and 5 also illustrate other superconductive features: Most notable is the irreversible magnetization associated with increasing versus decreasing magnetic field. During the experiment, the field sweep was periodically stopped, which produced the vertical spikes on the magnetization curves. This is attributed to flux creep in the materials. From the irreversible magnetization, we have calculated values for the critical current density  $J_c$  using the critical state model<sup>10</sup> of superconductivity. For  $\text{Ho}_1\text{Ba}_2\text{Cu}_3\text{O}_z$  at 4.2 K, we obtain an approximately constant  $J_c$  of  $5 \times 10^3$  A/cm<sup>2</sup> for  $20 < H < 80$  kOe. At 20 K,

the corresponding value is  $1.3 \times 10^3$  A/cm<sup>2</sup>. A more complete account of these results will be presented elsewhere.

In conclusion, we find from magnetization studies on HoBa<sub>2</sub>Cu<sub>3</sub>O<sub>z</sub> that the paramagnetic Ho subsystem and superconductive layers are highly decoupled from one another. Thus these materials constitute a highly anisotropic class of superconductive compounds.

*Note added.* In band-structure calculations, Mattheiss and Hamann (to be published) have found that the Y layer "effectively forms an insulating tunneling barrier." This theoretical result is consistent with the deductions from our experimental investigation and *visa versa*. Since then, experimental studies at IBM Yorktown on uniaxial

thin films have revealed the presence of critical current densities in the basal plane of Y<sub>1</sub>Ba<sub>2</sub>Cu<sub>3</sub>O<sub>z</sub> which are much higher than in polycrystalline materials.

We wish to acknowledge useful discussions with S. H. Liu, and the experimental assistance of Y. C. Kim, and to thank J. Brynstad who provided one of the Y-based samples used in this study. A portion of the work of one of us (J.R.T.) was supported by the Science Alliance. This research was sponsored by the Division of Materials Sciences, U.S. Department of Energy under Contract No. DE-AC05-84OR21400, with Martin Marietta Energy Systems, Inc.

<sup>1</sup>J. G. Bednorz and K. A. Müller, *Z. Phys. B* **64**, 189 (1986).

<sup>2</sup>See D. U. Gubser, R. A. Hein, S. H. Lawrence, M. S. Osofsky, D. J. Schrod, L. E. Toth, and S. A. Wolf, *Phys. Rev. B* **35**, 5350 (1987), and the accompanying papers; C. Politis, J. Geerk, M. Dietrich, and B. Obst, *Z. Phys. B* **66**, 141 (1987).

<sup>3</sup>C. W. Chu, P. H. Hor, R. L. Meng, L. Gao, Z. J. Huang, and Y. Q. Wang, *Phys. Rev. Lett.* **58**, 405 (1987).

<sup>4</sup>R. J. Cava, R. B. van Dover, B. Batlogg, and E. A. Rietman, *Phys. Rev. Lett.* **58**, 408 (1987).

<sup>5</sup>M. K. Wu, J. R. Ashburn, C. J. Torng, P. H. Hor, R. L. Meng,

L. Gao, Z. J. Huang, Y. Q. Wang, and C. W. Chu, *Phys. Rev. Lett.* **58**, 908 (1987).

<sup>6</sup>R. J. Cava, B. Batlogg, and R. B. van Dover (unpublished).

<sup>7</sup>L. F. Mattheiss, *Phys. Rev. Lett.* **58**, 1028 (1987); J. Yu, A. J. Freeman, and J.-H. Xu, *ibid.* **58**, 1035 (1987).

<sup>8</sup>W. Weber (private communication).

<sup>9</sup>Z. Fisk, J. D. Thompson, E. Zirngiebl, J. L. Smith, and S.-W. Cheong (unpublished).

<sup>10</sup>M. Tinkham, *Introduction to Superconductivity* (McGraw-Hill, New York, 1975), p. 171.